Supporting Material

This is an excerpt of M. J. Cairns, G. M. Barassi, T. Borrmann. Composites of nanostructured calcium silicate hydrate with superparamagnetic particles and their use in the uptake of copper from solution. Environmental Chemistry, 2014, 11 (3), 303. DOI: 10.1071/EN13183.

Experimental

General. Materials to produce NCSH were obtained from LobaChemie (calcium hydroxide AR grade), Orica Chemicals (sodium silicate N grade) and JaSol (technical grade hydrochloric acid). Water for all preparations was distilled prior to use.

For sorption tests, and for elemental analysis, analytical grade reagents were used for all work. Chemicals for this work were purchased from a variety of sources: Copper chloride from Ajax, nitric acid from APS, calcium carbonate from BDH, hydrochloric acid and sulfuric acid from LabScan, pH buffer solutions from Pure Science, copper nitrate and iron sulfate from Riedel-de-Haën.

Quantification of metal species was undertaken on a GBC906AA flame atomic absorption spectrometer. Prior to analysis, all samples were filtered through 0.45 μm cellulose membranes in order to remove any suspended solids. Calibration was performed with a minimum of 4 standard solutions. Each standard and sample was analysed in triplicate by the instrument, which also automatically prepared calibration curves. Where necessary, samples were diluted such that the analyte concentration was in the range covered by the standards. During the analysis, the calibration was checked every 10 samples by re- analysing a calibration standard, a blank solution and a sample. Analysis conditions used were those recommended by the instrument manufacturer, [1] which were consistent with other sources. [2]

X-ray Analysis. Powder X-ray diffraction patterns were collected using a Phillips PW 3710 MPD- controlled diffractometer. Typically, scans were recorded through an angular range of 6–70° 2θ at a scan speed of 0.020° 2θ s^{-1} using the Cu K_α spectral line. In cases where the XRD pattern was assigned to specific crystalline phases, reference patterns were taken from the ICDD Powder Diffraction File Version 4.41 and were of either Star or Indexed quality.

Particle Size Analysis. Particle size distributions were determined using a Malvern Mastersizer Hydro 2000 MU. Preferentially, the particle size distributions of NCSH samples were measured of slurries (powders suspended in water) or filter cake samples. Ultrasonication was performed for 30 seconds to ensure complete dispersion of the sample prior to data collection. The instrument software processed raw data such that a number-weighted size distribution was calculated, based on the average of three measurements.

Electron Microscopy. Electron microscopy was performed on a JEOL JSM 6500F field emission scanning electron microscope. Prior to analysis, samples were adhered to carbon tape on aluminium stubs and sputter-coated with a 4 nm thick Pt layer. The same instrument was used to record both electron micrographs and energy dispersive X-ray spectra (EDS).

Surface Area Analysis. Single point BET surface area determinations were undertaken with the use of a Mircomeritics FlowSorb II 2300 instrument, using a gas mixture of 29.1 vol% N_2 in He. [3]

pH. pH-values were measured using a HANNA Instruments 5521 meter or a EuTech Instruments CyberScan pH 11 meter.

X-Ray Photoelectron Spectroscopy. XPS measurements were undertaken on a Kratos Axis Ultra XPS instrument located at Auckland University. The Al K_α X-ray source was provided by a filament operating at 10 mA and 15 kV. Prior to analysis, samples were mounted on carbon tape, which was used as the internal standard, with the C 1s peak adjusted to a binding energy of 285 eV. Data analysis was performed with the fityk program. [4]

Magnetometry. Magnetisation of γ-Fe_2O_3-NCSH composite materials was measured on an Alternating Gradient Magnetometer, model 2900 (Princeton Measurements Corporation). A known mass of sample (a few milligrams) was packed into a glass capillary tube, the ends of which were sealed with glue to prevent sample movement within the tube. Silicone grease was used to mount the sample on the instrument's sample probe. Magnetisation curves were recorded at a scan rate of 8 kA m^{-1} s^{-1} between +800 kA m^{-1} and −800 kA m^{-1}.

General Synthetic Procedure. NCSH was prepared using a batch process. Typically batches of between 200–500 cm^3 were prepared. The following relates to the preparation of a sample at a reaction volume of 500 cm^3, giving approximately 10 g (dry basis) of calcium silicate:

In a plastic beaker, $Ca(OH)_2$ (78.1 mmol, 5.79 g), was suspended in 250 cm^3 of 0.174 mol dm^{-3} HCl under vigorous mixing provided by a mechanical overhead stirrer (either a Heidolph RZR 1 or an IKA-Werke Eurostar Digital). In a separate plastic beaker sodium silicate (15.91 g of 27 wt % SiO_2, 71.5 mmol) was diluted to 250 cm_3 with H_2O. This provided precursor solutions with the following equivalent concentrations: [Ca] = 0.312 mol dm^{-3} and [SiO_2] = 0.286 mol dm^{-3}.

The sodium silicate solution was rapidly added to the calcium hydroxide suspension, immediately generating a viscous slurry. Stirring of the resulting calcium silicate precipitate was maintained for about one hour. Then the material was aged by allowing it to stand overnight. Various post-synthesis treatments were applied, depending on the requirements for the final material.

Filter-cake. If it was deemed necessary to maintain the pore structure, and hence accessible surface area, the filter cake was stored in a sealed container and not permitted to dry out. The solids content of a subsample was determined by taking a known mass of the filter-cake (10 to 20 g) and drying it at 110 ◦C overnight in an oven. Typically, samples were found to contain between 5 and 15 wt % solids.

Water Washed Material. It has previously been shown that drying the silicate leads to collapse of the pore structure, resulting in a significantly reduced surface area. If such a silicate was desired, the as-made material was recovered by vacuum filtration, and the filter cake washed thoroughly with water. Then the filter cake was dried in an oven at 110 ◦C overnight. [5]

2-Ethoxyethanol Washed Material. In some cases, it was necessary to dry the material while maintaining the high surface area. In this case, 2-ethoxyethanol was used as a spacer compound due to its low surface tension compared to H_2O. During the filtration step, the filter cake was first washed well with water to remove any salts (Na^+ and Cl^- are spectator ions in the calcium silicate precipitation reaction). After the final water rinse, but before suction through the filter cake was lost, one plug volume of 2-ethoxyethanol was added to the filter funnel. It was allowed to pass through the filter cake, displacing any water present. The filter cake was subsequently dried in a vented oven at 110 ◦C. Due to the higher boiling point of 2- ethoxyethanol, when compared to water, it took longer to dry the 2-ethoxyethanol washed filter-cake than to dry the water washed one. Typically, samples were dried for at least two days prior to use.

Magnetite. Magnetite nanoparticles having a nominal diameter of 15 nm were prepared according to the method of Berger, [6] itself based on the co-precipitation method of Massart. [7] The iron salts $FeCl_2{\cdot}4H_2O$, 10.53 g (0.053 mol), and $FeCl_3{\cdot}6H_2O$, 28.65 g (0.106 mol), were dissolved in 132.5 cm_3 of 2 mol dm^{-3} HCl, providing a solution 0.40 mol dm^{-3} in Fe^{2+} and 0.80 mol dm^{-3} in Fe^{3+}. Ammonia solution (1 mol dm^{-3}, 1325 cm^3) was added drop wise to the rapidly stirred iron solution over the course of six hours. The addition of NH_3 caused the formation of a fine black Fe_3O_4 suspension. The reaction mixture was stirred for a further 30 minutes after completion of the NH_3 addition. The magnetite was precipitated by placing a rare-earth magnet under the reaction flask, and the supernatant decanted off. The magnetite was re-suspended in 500 cm^3 of water, and the precipitation step repeated until the magnetite had been rinsed four times, at which point the supernatant had a pH value of approximately 7. The magnetite was finally suspended in 500 cm^3 water and the solids content determined by drying a subsample on a rotary evaporator.

Magnetite-Calcium Silicate Composite. For the preparation of composite materials containing magnetite, the NCSH was assumed to have an empirical formula of $Ca_{0.8}SiO_{2.8}{\cdot}2H_2O$, which was used to determine the mass ratio of magnetite to silicate. For example, to synthesise a material containing 25 wt% Fe_3O_4, magnetite (3.36 g, 14.5 mmol) was added to a sodium silicate solution as detailed in the general procedure. The mixture was blended with a stirring rod for five minutes in order to ensure that the Fe_3O_4 was thoroughly

dispersed. At this point, the magnetite-containing sodium silicate solution was added to the calcium hydroxide suspension as per the general synthetic procedure. Once the material had aged overnight, post-synthesis treatments such as reinforcement or 2-ethoxyethanol washing could be carried out. If large quantities of the material were desired (a total reaction volume greater than 500 cm^3), the magnetite was dispersed in the sodium silicate solution via the use of a mechanical overhead stirrer equipped with a plastic mixing blade. This method proved suitable for the synthesis of composites ranging from 1–25 wt% Fe_3O_4, without significantly degrading the accessible surface area of the silicate. Attempts were not made to synthesize composites containing a greater percentage of Fe_3O_4. To generate powdered samples the composite filter cake was dried under nitrogen at 110 °C or freeze-dried.

Results and Discussion

Nanostructured calcium silicate hydrate (NCSH) formed smooth, homogeneous appearing suspensions with a Fe_3O_4 precursor, which was added to the silicate during its synthesis. The post-treatment of the suspensions proved to be crucial in terms of the magnetic properties of the composites generated. Depending on the drying method a NCSH composites containing magnetite (**1**) or maghemite (**2**) could be synthesized. If the suspension was not dried and just filtered to yield a grey sorbent filter cake, was freeze dried or dried in absence of air, a magnetite composite (**1**) was prepared. However, upon following the standard NCSH synthesis procedure and drying the composite in air at 110 °C for 2 days the magnetite was oxidized to maghemite (γ-Fe_2O_3). [5] This was evidenced by a change in color from grey to brown and could be confirmed by X-ray diffraction (**Figure S1**). The reflections could be identified to belong to the pattern of maghemite, NCSH (or a calcite impurity – see literature [8]) and the sample holder employed. Reflections associated with magnetite could only be observed in the samples, which were not at 110 °C dried under air. Although even in those samples it was difficult to decide whether maghemite, magnetite or a mixture were present as the patterns overlap to a large degree. Based on the low angle diffractions and the coloration of the samples these composites were considered to contain magnetite (Fe_3O_4).

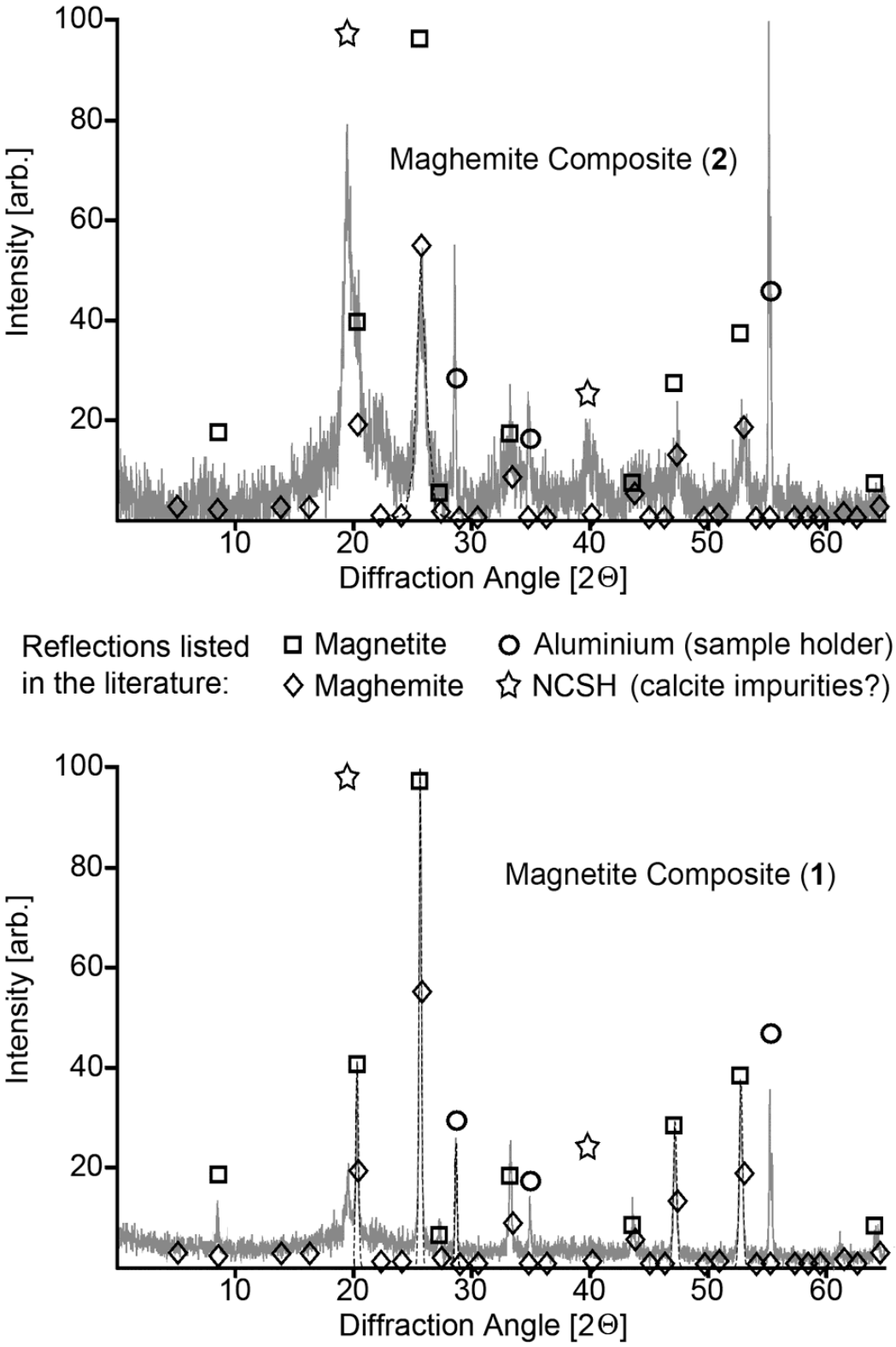

Figure S1. X-ray diffraction pattern of composites containing magnetite, Fe_3O_4-NCSH, (**1**), and maghemite, γ-Fe_2O_3-NCSH, (**2**).

The particle size of the magnetite particles used for the preparation of the composites was estimated using the Scherrer formula, relating the X-ray diffraction linewidth to size of the crystalline domains within a particle following

the relation $t = 0.9\lambda (B \cos(\theta))^{-1}$ in which t is the particle diameter, λ is the wavelength of incident X-ray radiation, and B is the thickness of the diffraction peak centered at an angle θ. The four most intense diffraction peaks assigned to magnetite have been modeled with Gaussian functions ($f(x) = h \exp(-\ln(2)(x-c)^2 w^{-2})$, where h is the peak height, c its centre and w its half width at half median height). Parameters of these functions are given in Table 1. Analysis of the four most intense diffraction peaks indicated a particle diameter in the range of 13–20 nm. This is within the reported size range for magnetite particles synthesized in a similar manner to the synthesis methods used here. [6] Particles with this diameter are at the boundary between ferrimagnetic and superparamagnetic behavior. [9] A measurement of the remnant magnetization showed that the precursor particles, the magnetite composite, Fe_3O_4-NCSH (**1**), and the magnetite containing composites, *γ*-Fe_2O_3–NCSH (**2**), were superparamagnetic; no hysteresis loop was observed in the measurement of the magnetic moment. The saturation magnetic moment of the precursor was found to be lower (53 A m^2 kg^{-1}) than expected for a pure *γ*-Fe_2O_3phase (90 A m^2 kg^{-1} [9]). Consequently, the magnetite content of the precursor material was estimated to be around 58 wt%. The residual mass (42 wt%) was attributed to the possible formation of an antiferrimagnetic *α*-Fe_2O_3 phase present as an impurity within the samples. Using the magnetite content of the precursor as base value an expected saturation magnetic moment of 42 A m^2 kg^{-1} was estimated for the maghemite in the corresponding composite (**2**). The superparamagnetic nature of the composites could be confirmed by observation of their settling behavior (**Figure S2a and S2b**).

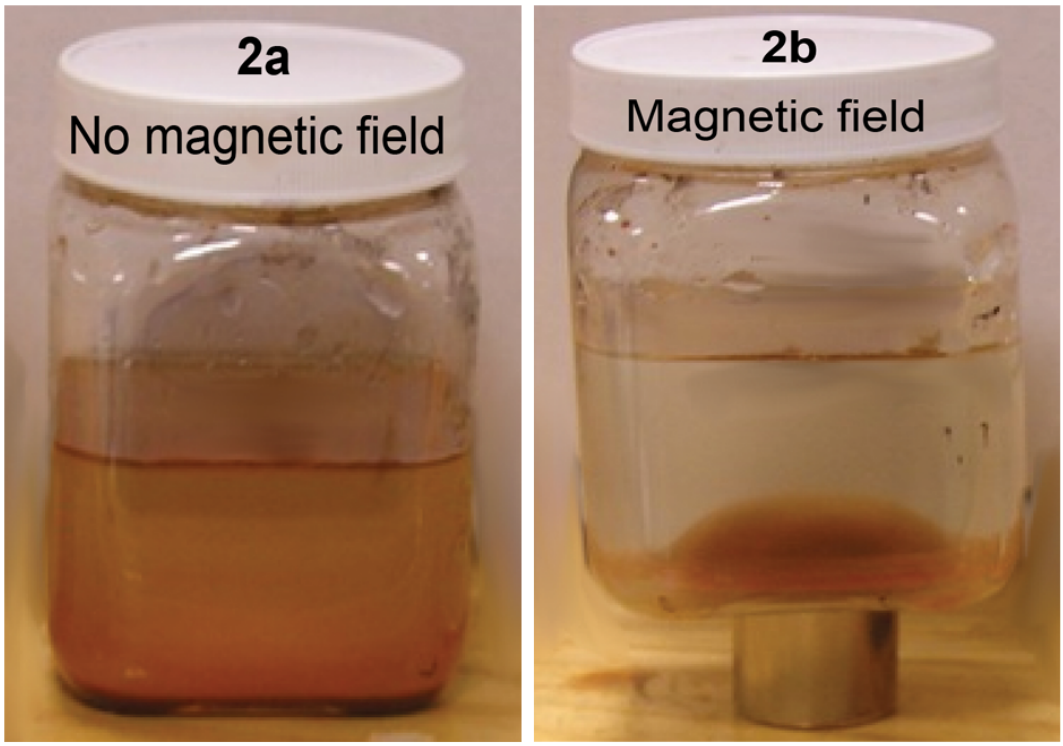

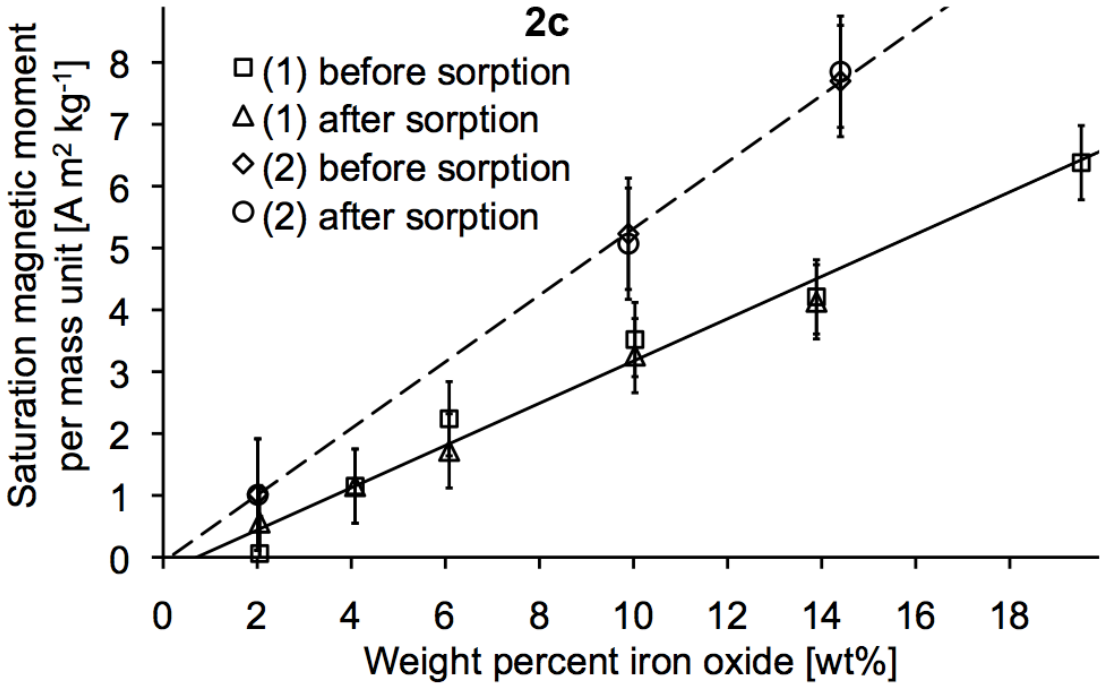

Figure S2. Settling behavior of γ-Fe_2O_3–NCSH composite (**2**) suspended in water. **a**. Absence of a magnetic field. **b**. Presence of a magnetic field. **c**. Measurement of the saturation magnetic moment of the Fe_3O_4-NCSH composite, (**1**), and the γ-Fe_2O_3–NCSH composite, (**2**).

Magnetic particles would have started to flocculate and settle spontaneously within seconds of a sample being allowed to rest. It was shown that the composites produced did settled similarly slowly as the untreated NCSH in the absence of an external magnetic field (**Figure S2a**). However, if a magnet

was placed next to or underneath a container, the composites flocculated rapidly – within seconds (for example composite (**2**) shown in **Figure S2b**) and settled in the container in closest proximity to the magnet. This indicated the possibility of employing the composites in a High Gradient Magnetic Separation. Furthermore the amount of iron oxide contained in the composite appeared to be in a linear relationship to the magnetic moment of the sample (**Figure S2c**). This means that the magnetic separation could be controlled partially over the amount of superparamagnetic component used in the making of the sorbent composite. Extrapolation of the saturation magnetic moment data showed that the magnetite component of the composite (**1**) had a magnetic moment of about 53 A m^2 kg^{-1} comparable to that of the precursor. However, extrapolating the data for the maghemite component of composite (**2**) correspondingly showed that the maghemite component had only a magnetic of about 34 A m^2 kg^{-1} well short of the estimated 42 A m^2 kg^{-1}. This indicated that only about 80 wt% of the magnetite was converted to maghemite and that the maghemite component of composite (**2**) had a purity of only about 43 wt%. A comparison of the magnetic moment data for the composites prior to the uptake of copper and after sample recovery showed that no difference between samples within the margin of error. This meant that uptake of copper into the composites did not change the magnetic properties of the sorbent.

Particle Size Analysis. The particle size distribution for a series of composites prepared from a Fe_3O_4 suspension along with the distributions of the starting materials, NCSH and Fe_3O_4 were collected (**Figure S3**). [5] With an average of about 0.4 µm the particle size distribution (**Figure S3a** 100 wt% sample) of the pure Fe_3O_4 precursor particles was far higher than the one calculated from the X-ray diffraction results earlier. The Scherrer calculation indicated the presence of 15 µm diameter particles. A practical test showed that the particles in suspension could pass cleanly through a 0.45 µm filter membrane. It is likely that the precursor particles agglomerated during the particle size measurements; therefore, the results have to be treated with caution. It is likely that some distributions were representing aggregates rather than discreet particles.

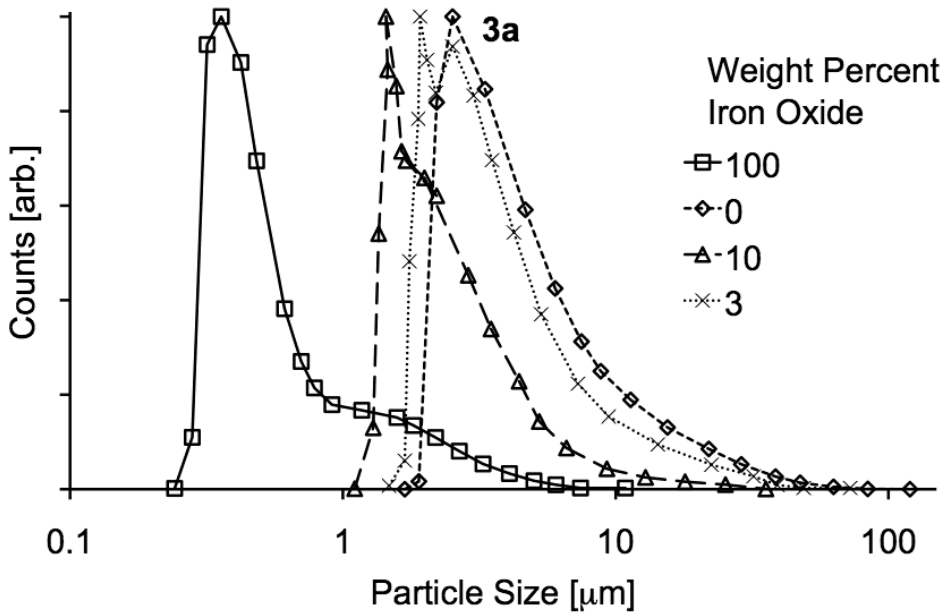
3a
Weight Percent
Iron Oxide
100
0
10
3
Counts [arb.]
0.1
1
10
100
Particle Size [μm]

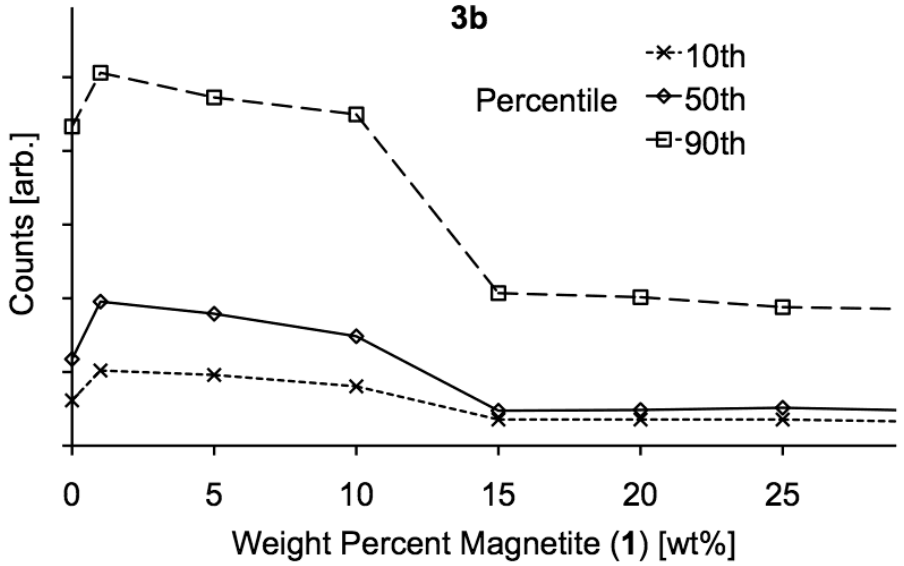
3b
Percentile
10th
50th
90th
Counts [arb.]
0
5
10
15
20
25
Weight Percent Magnetite (1) [wt%]

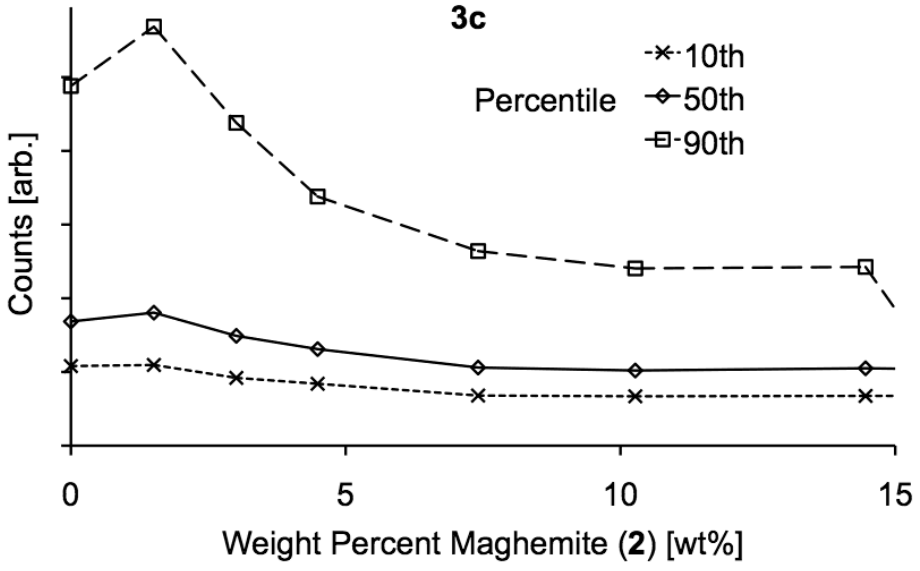
3c
Percentile
10th
50th
90th
Counts [arb.]
0
5
10
15
Weight Percent Maghemite (2) [wt%]

Figure S3. Particle Size Measurements. **a**. Particle size distributions for pure NCSH (0 wt% sample), pure Fe_3O_4 precursor (100 wt% sample) and two composites (**2**) containing 3 and 10 wt% Fe_3O_4. **b**. Comparison of key parameters for the particle size of magnetite composites (**1**) containing increasing amounts of magnetite. **c**. Corresponding comparison of key parameters for maghemite composites (**2**) with increasing amounts of maghemite.

The shape of all investigated particle size distributions was very similar except for the samples with low contents of magnetic particles, where a secondary maximum at the position of pure NCSH could occur. A representative distribution for an iron oxide content of 3 wt% magnetite is shown in **Figure S3a**. The secondary maximum indicated that some NCSH was formed, which was not associated with magnetic particles. The secondary maximum disappeared for higher contents of iron oxide and was no longer observed for iron oxide contents of 10 wt% (**Figure S3a**) indicating that the particles formed are homogeneous.

To allow for an easier comparison of the distributions their key parameters, the 10^{th}, 50^{th} and 90^{th} percentiles, were plotted against the content of iron oxide particles (composites containing Fe_3O_4 (**1**) in Figure 3b and those with γ-Fe_2O_3 (**2**) in **Figure S3c**). Concentrations of the precursor calcium hydroxide and sodium silicate solutions were [Ca] = 0.624 mol dm^{-3} and [SiO_2] = 0.572 mol dm^{-3}. The addition of magnetite into the NCSH structure did not have a significant effect on the particle size of the resultant composite. As the magnetite content of the composite was increased, its particle size decreased. This would be expected should the magnetite be providing additional nucleation sites for the NCSH. The additional nucleation sites would cause an increase in the rate of nucleation, meaning that a greater number of smaller particles would be formed from a given amount of reagents. The decrease in particle size set on later for the γ-Fe_2O_3-NCSH composites (**2**) hinting again at agglomeration of the particles. Prior research has shown that agglomeration of NCSH is strongly dependent on the concentration of the material and the experimental setup. Consequently, it should be feasible to avoid agglomeration in real life applications of the composites. However, the effect of agglomeration of NCSH and composites and its effects (diffusion and such) will be investigated in future studies.

Surface Area. The variation in surface area for the γ-Fe_2O_3-NCSH (**2**) composite materials is shown in **Figure S4**. As expected, the 2-ethoxyethanol washed materials possessed a significantly greater surface area than the water washed composites. The range of surface area was within that expected for a typical non-composite NCSH (150 ± 50 m^2 g^{-1} for water washed materials and 500 ± 100 m^2 g^{-1} for the 2-ethoxyethanol materials). [5] As the γ-Fe_2O_3 content of the composite materials increases, the surface area rapidly increases and then slowly decreases. The decrease in surface area with increasing γ-Fe_2O_3 content may be explained by considering that addition maghemite leads to an increase in the density of the NCSH composite. As such, the specific surface area will decrease. The observed surface area increase at low γ-Fe_2O_3 content has a less obvious origin. It is probable that

the presence of the maghemite crystallites provides for additional nucleation sites during the synthesis of the NCSH composite. This would lead to the formation of smaller NCSH particulates, having a higher surface area to volume ratio, and hence a higher absolute surface area. At low maghemite content, the higher surface area to volume ratio would outweigh the diminutive effect of the increased mass on the specific surface area. The increase in specific surface area at low γ-Fe_2O_3 content is consistent with the decrease in particle size observed earlier. The results for the Fe_3O_4 containing composites were comparable.

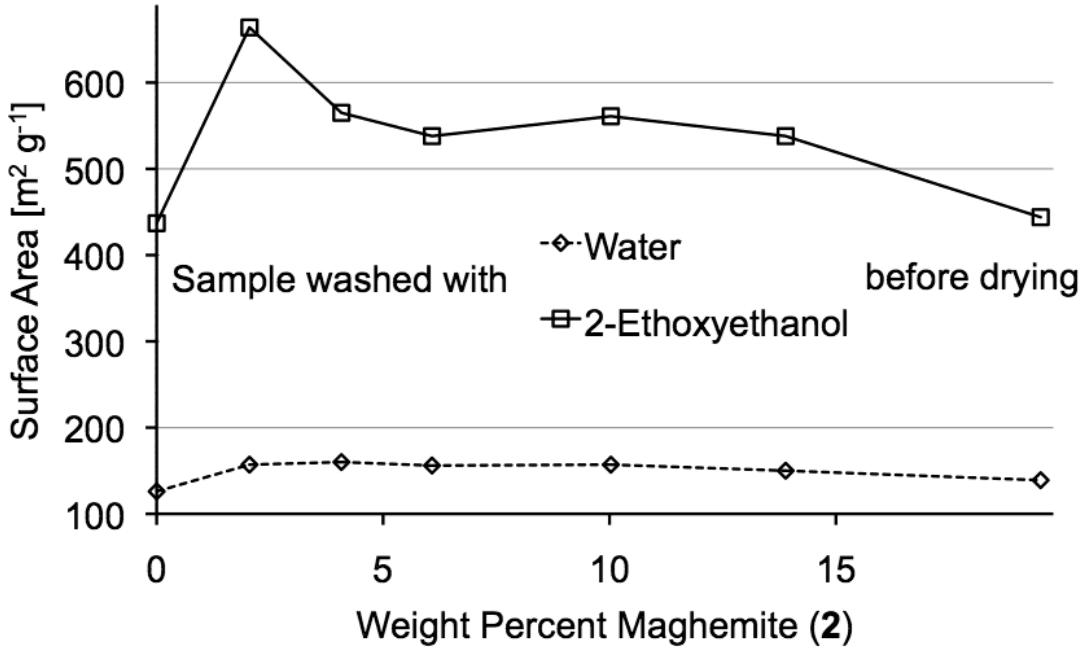

Figure S4. Comparison of surface area for water and ethoxyethanol washed maghemite composites (**2**) with a variation in the maghemite content.

Scanning electron microscopy showed that the composites appeared very similar to NCSH reported in the literature in terms of its surface morphology (**Figure S5a**-**c**). The typical desert rose resembling nanostructure was observed. No iron could be detected within the composite materials in X-ray Photoelectron Spectroscopy (XPS) studies, indicating that the magnetite and maghemite particles were incorporated within the NCSH structure, and not simply bound to the surface of the material. Energy dispersive spectroscopy (EDS) with its greater sample penetration depth (micrometer scale compared to picometer scale for XPS) provided evidence for a uniform iron distribution within the composites (X-ray map generated from EDS **Figure S5d**).

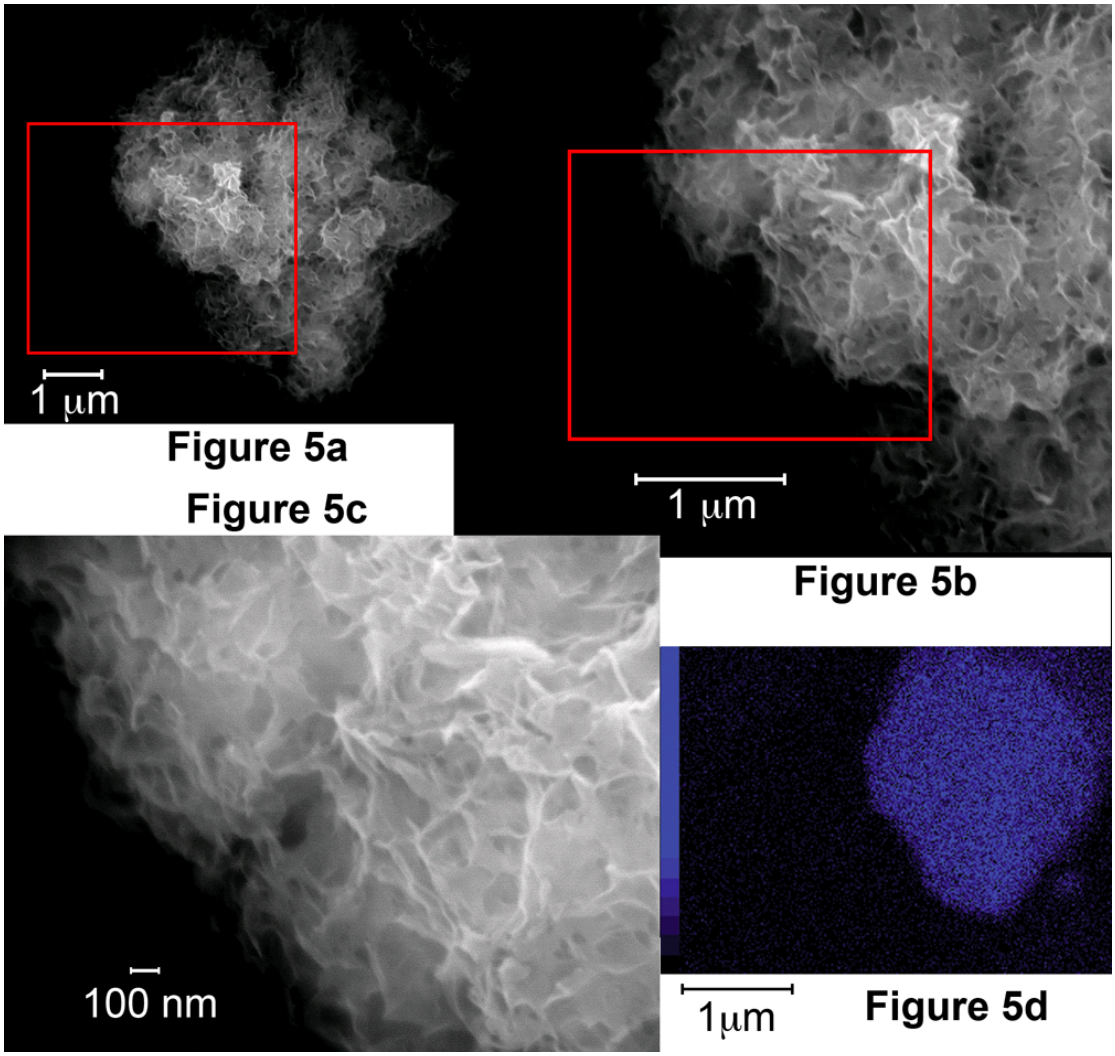

Figure S5. Electron microscopy. **a**-**c**. Scanning electron microscope images of maghemite composite (**2**) containing 10 wt% maghemite. **d**. X-ray map generated from energy dispersive spectrum of the composite showing distribution of iron in the sample.

[1] H.-N. Chou, C. A. Naleway, Extraction-spectrophotometric determination of trace phosphorus in chromium-bearing materials which may contain silica, niobium, tantalum, zirconium, titanium, and hafnium, *Analytical Chemistry* **1984**, *56*, 1737–1738.
[2] N. Athanasopoulos, Flame Methods Manual for Atomic Absorption; *GBC Scientific Equipment Pty. Ltd.* **1989** (Dandenong, Vic. Australia).
[3] Flowsorb II 2300 Instruction Manual for Determining Single Point and Multipoint Surface Area, Total Pore Volume, and Pore Area and Volume Distribution, *Micromeritics Instrument Corporation* **1990** (Norcross, GA, U. S. A.).
[4] M. Wojdyr, fityk Version 0.8.2 *http://www.unipress.waw.pl/fityk/* **2008**.
[5] A. J. McFarlane, The Synthesis and Characterisation of Nanostructured Calcium Silicate, *Ph.D. thesis, Victoria University of Wellington* **2008**.
[6] P. Berger, N. B. Adelman, K. J. Beckman, D. J. Campbell, A. B. Ellis, G. C. Lisensky, Preparation and Properties of an Aqueous Ferrofluid*, Journal of Chemical Education* **1999**, *76*, 943–948.

[7] R. Massart, Preparation of aqueous magnetic liquids in alkaline and acidic media, *IEEE Transactions on Magnetics* **1981**, *MAG-17*, 1247–1248.
[8] T. Borrmann, J. H. Johnston, A. J. McFarlane, K. J. D. MacKenzie, A. Nukui, Structural elucidation of synthetic calcium silicates, *Powder Diffraction* **2008**, *23 (3)*, 204- 212.
[9] D. J. Dunlop, Superparamagnetic and single-domain threshold sizes in magnetite, *Journal of Geophysical Research*